International Journal of Mass Spectrometry 307 (2011) 240–244

Contents lists available at ScienceDirect

International Journal of Mass Spectrometry

journal homepage: www.elsevier.com/locate/ijms

Element imaging in formalin fixed slices of human mesencephalon

Andreas Matusch[b,*], Andreas Bauer[b,c], J. Sabine Becker[a]

[a] Central division of Analytical Chemistry, Research Centre Jülich, 52425 Jülich, Germany
[b] Institute of Neurosciences and Medicine (INM-2), Research Centre Jülich, 52425 Jülich, Germany
[c] University Duesseldorf, Medical Faculty, Department of Neurology, 40225 Duesseldorf, Germany

ARTICLE INFO

Article history:
Received 13 November 2010
Received in revised form 14 March 2011
Accepted 14 March 2011
Available online 23 March 2011

Keywords:
Human brain tissue
LA-ICP-MS bioimaging
Metal imaging
Quantitative distribution analysis
Substantia nigra

ABSTRACT

The scarcity of native frozen pathological and healthy human brain tissue is actually one of the major bottlenecks concerning the investigation of neuropsychiatric diseases. Therefore it is of some interest to make formalin fixed tissue specimens accessible to mass spectrometric analytical techniques. Laser ablation inductively coupled plasma mass spectrometry (LA-ICP-MS) and matrix matched standards were employed to generate quantitative element maps of human mesencephalon slices that had been stored in formalin for more than 10 years of a single subject. The characteristic distribution patterns of Cu and Zn were completely blunted but Fe was clearly enriched in the substantia nigra (SN) – especially in the matrix of the pars compacta – and the nucleus ruber (NR) at concentrations of 179 $\mu g\,g^{-1}$, 231 $\mu g\,g^{-1}$ and 187 $\mu g\,g^{-1}$ (wet weight), respectively, very similar to literature values obtained from homogenates of fresh tissue. Mn and Ca congruently reflected the distribution of melanised SN neurons. Interestingly, the distribution of Pb was congruent to that of Fe reaching 0.8 $\mu g\,g^{-1}$ in the SN, 1.1 $\mu g\,g^{-1}$ in the matrix and 0.9 $\mu g\,g^{-1}$ in the NR. Images of C and P reflected the gray matter-white matter partition of the tissue. These results suggest that a meaningful quantitative assessment of Fe, Mn and Pb is possible in tissue samples which have previously been stored in buffered formalin solution.

1. Introduction

Storage of tissue specimens in (most commonly 4% buffered) formalin solution implicates the cross linkage of macromolecules and a wash-out and homogenous distribution of soluble species such as Zn^{2+}, Na^{+} and Mg^{2+}. This restricts the suitability of formalin fixed samples for chemical analysis. However, the systematic acquisition and collection of cryo-preserved material in the realm of brain banks is an ongoing process. Notwithstanding, formalin fixed brain specimens of series of tens to several hundreds of cases of neuropsychiatric diseases are available in neuro-pathological collections. Therefore, some efforts have been undertaken to adapt mass spectrometric imaging and "omics" techniques to formalin fixed samples and to assess the feasibility and validity of these determinations [1].

Metal concentrations in the human mesencephalon have so far been measured in acidic digests of tissue homogenates. Non- or semi-quantitative imaging studies on tissue stored in formalin used X-ray fluorescence [2] and Prussian blue stains for Fe [3] which does not detect heme-Fe or Fe in melanised neurons. High resolution techniques obtained quantitative images of single cells [4] but not average concentrations throughout regions of several mm.

The SN consists of two subdivisions, pars reticulata containing fibers and loosely packed cells and pars compacta (SNpc) containing dense clusters of melanised cell bodies. In healthy subjects iron was shown to accumulate in the SNpc with growth and to maintain a stable concentration between 20 and 90 years of age [5]. In Parkinson's disease increased iron concentrations were observed in the SNpc [6].

The relatively new technique of bioimaging LA-ICP-MS has been described in detail in several previous publications [7–13] and is also dealt with in some other articles in this special issue. The aim of the present pilot and feasibility study on a single subject was to assess, which information can be gathered by LA-ICP-MS bioimaging of formalin fixed human mesencephalic tissue.

2. Experimental

2.1. Sample and sample preparation

The present sample originates from a 72-year-old man, who had no neurological symptoms in his medical history and died because of non-neurological pathology. The post mortem delay was <24 h and the medication was not known. The brain was pre-fixed in 4% formalin. Cryo-sections of 100 μm thickness were obtained from

* Corresponding author. Fax: +49 2461 61 2161.
E-mail address: a.matusch@fz-juelich.de (A. Matusch).

1387-3806/$ – see front matter © 2011 Elsevier B.V. All rights reserved.
doi:10.1016/j.ijms.2011.03.006

selected regions and stored in buffered formalin solution. Upon macro- and micropathological criteria including advanced silver stains for neurofibrillary tangles and amyloid using the methods of Gallyas and Campbell [14] and immuno-histochemical stains using antibodies against alpha synuclein [15], the brain had been categorized at stage III with respect to neurofibrillary tangles of Alzheimer type (stages I–VI) [14] and normal (zero) with respect to Aβ- [14] and Lewy [15] pathology (stages A–C and 1–6, respectively).

100 μm thick formalin fixed sections were mounted onto glass slides without additional adhesive measures and photomicrographs were taken. A line by line laser ablation of the tissue was impossible as it fissured and fragmented into fine pieces detaching from the glass surface. This occurred despite the use of StarFrost® adhesive slides which, out of a series of commercial slide products, enable the strongest adhesion. It was therefore necessary to glue the tissue onto the slide. For this purpose, the tissue was dehydrated in a series of isopropanol bathes of increasing concentrations (70%, 95% and 100%) followed by xylene bathes (at least 3 h each) and finally immersed for 1 day in a viscous 30% dilution of DePeX (a neutral solution of polystyrene and plasticizers in xylene from Serva, Heidelberg, Germany) in xylene. A drop of DePeX was placed onto a slide, then the section was spread using a brush of semi rigid synthetic fibers (DaVinci Nova Synthetics Series 1570, size 3 from Defet, Nürnberg, Germany). During the drying and curing process the section was once again wetted with the 30% DePeX dilution. The plain of the two neighbouring sections of a piece of mesencephalon and its localization is indicated in Fig. 1.

Matrix matched standards were obtained by homogenization of pieces of the frontal lobe of the same brain, stored in the same formalin solution, addition of 0, 5, 11, 53, 78 and 105 $\mu g\,g^{-1}$ of Fe (10.000 $\mu g\,g^{-1}$ standard solution, NBS) and by a factor of ten lower amounts of Al, Mn, Cu, Zn, Cd, Hg and Pb (1000 $\mu g\,g^{-1}$ standard solution, Merck), thorough mixing, freezing in a mould and cutting of 100 μm thick cryo-sections.

2.2. Instrumentation, image generation and image analysis

Standards and samples were placed together in the ablation chamber of a commercial laser ablation (LA) system (New Wave UP 266, Fremont, CA, USA) coupled to a quadrupole inductively coupled plasma mass spectrometer (XSeries2, Thermo Fisher Scientific, Germany). The laser ablation system was operated with a frequency-quadrupled Nd:YAG laser at a wavelength of 266 nm, a repetition frequency of 20 Hz and a laser spot diameter of 120 μm. The samples were ablated line by line (scanning mode) at laser energy of 0.08 mJ, 20 Hz repetition frequency, 60 $\mu m\,s^{-1}$ scan speed and 2.65 s acquisition time per data point corresponding to 160 μm *x*-distance. The distance between two ablated lines was 170 μm (centre to centre). Thus, in this experiments no oversampling was used [16]. Argon was used as carrier gas that transported the ablated material into the inductively coupled plasma source (ICP). The ions formed in the ICP were extracted into a quadrupole-based mass spectrometer and separated according to their mass-to-charge ratio. The maximum ion intensity of analytes was observed at a carrier gas flow rate of 0.86 $L\,min^{-1}$. The ICP was operated with an Rf power of 1500 W.

Images were reconstructed by alignment of the continuous list of raw pixel data into lines using in-house written software (LA-ICP-MS-ImageGeneration, v5). Element images were coregistered to photomicrographs and calibrated using Pmod 3.0 (Pmod, Zürich, Switzerland). With the same software average concentrations in free hand drawn regions of interest (ROIs) were read out. The procedure of quantitative bioimaging of elements using LA-ICP-MS in native tissue with emphasize on brain samples has been described in previous publications [7,9–11,13] and was refined and adapted to the particular type of sample here.

Table 1
Element concentrations referred to wet weight averaged over selected regions of interest in two neighbouring sections of a human mesencephalon stored in formalin.

$\mu g\,g^{-1}$	Region	Section No	
		1	2
Fe	*Precision*[a]	±2	±6
	Entire section	136	140
	Substantia nigra (total)	171	188
	SN pars reticularis	103	119
	SN pars compacta	207	179
	SNpc Matrix/anterior part	220	242
	SNpc nigrosomes/posterior part	164	165
	Nucleus ruber	186	188
	Pedunculus cerebri	120	121
	Central gray	134	111
	Other tegmentum mesencephali	94	94
Mn	*Precision*[a]	±0.2	±0.4
	Entire section	0.6	1.4
	Substantia nigra (total)	0.6	1.7
	SN pars reticularis	0.6	1.4
	SN pars compacta	0.6	1.8
	SNpc cell rich areas	0.7	2.1
	SNpc cell poor areas	0.6	1.6
	Nucleus ruber	0.6	1.6
	Pedunculus cerebri	0.6	1.3
	Other tegmentum mesencephali	0.6	1.4
Pb	*Precision*[a]	±0.3	±0.2
	Entire section	0.6	0.6
	Substantia nigra (total)	0.7	1.0
	SN pars reticularis	0.4	0.5
	SN pars compacta	0.8	1.2
	SNpc Matrix/anterior part	0.9	1.3
	SNpc nigrosomes/posterior part	0.6	0.9
	Nucleus ruber	0.7	1.0
	Other tegmentum mesencephali	0.5	0.4
Cd	*Precision*[b]	±0.01	±0.01
	Entire section	0.1	0.1

[a] The precisions was obtained from the respective calibration curves of matrix matched standards and corresponds to 7 mm^2 of ablated tissue section equalling the smallest region.
[b] Precision for 143 mm^2 corresponding to the entire area.

3. Results and discussion

3.1. Element distribution patterns

Anatomically informative distribution patterns of C, P, S, Ca, Mn, Fe, Ni and Pb were obtained. The images of the isotopes measured of a given element were almost identical, such as of ^{24}Mg and ^{25}Mg; ^{56}Fe and ^{57}Fe; ^{63}Cu and ^{65}Cu; ^{64}Zn and ^{66}Zn, respectively. The isotopes ^{44}Ca, ^{56}Fe, ^{63}Cu, ^{64}Zn, ^{60}Ni, ^{111}Cd and ^{208}Pb were selected for calibration or illustration. Calibration curves with $R > 0.99$ were obtained from all elements added to the standard homogenates in both of two measurements except for one of the two Zn measurements were it was 0.987. Fig. 2 shows a photomicrograph, the element images obtained from the neighbouring sections 1 and 2 each with the set of ROIs superimposed and overlays of photomicrograph and element maps. Regional element concentrations are given in Table 1. All concentrations given in this article refer to wet weight of tissue. Cu and Zn distributions which display distinct gray matter-white matter partition in native tissue were completely blunted from the present tissue specimen.

3.2. Metal concentrations—comparison to previous data and persistence

The average Fe concentration of 179 $\mu g\,g^{-1}$ in SN (total, SNpc and SNpr) measured by LA-ICP-MS was very similar to those concentrations published for acidic digests of homogenates of fresh

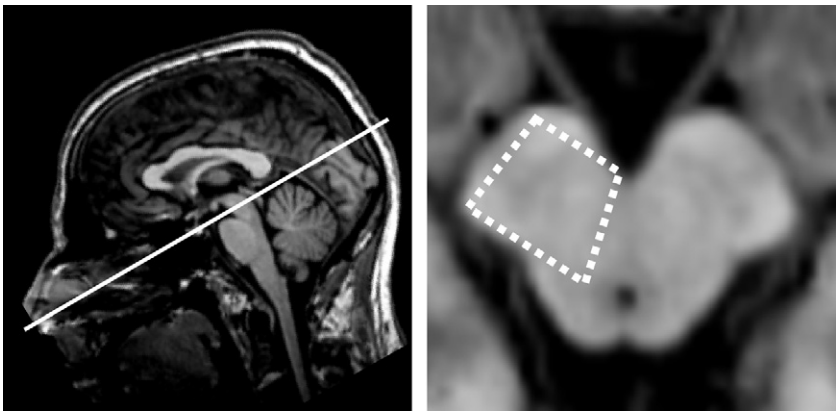

Fig. 1. Plain and position of the two present mesencephalon sections are outlined on a magnetic resonance image (T1 weighted MPRAGE sequence).

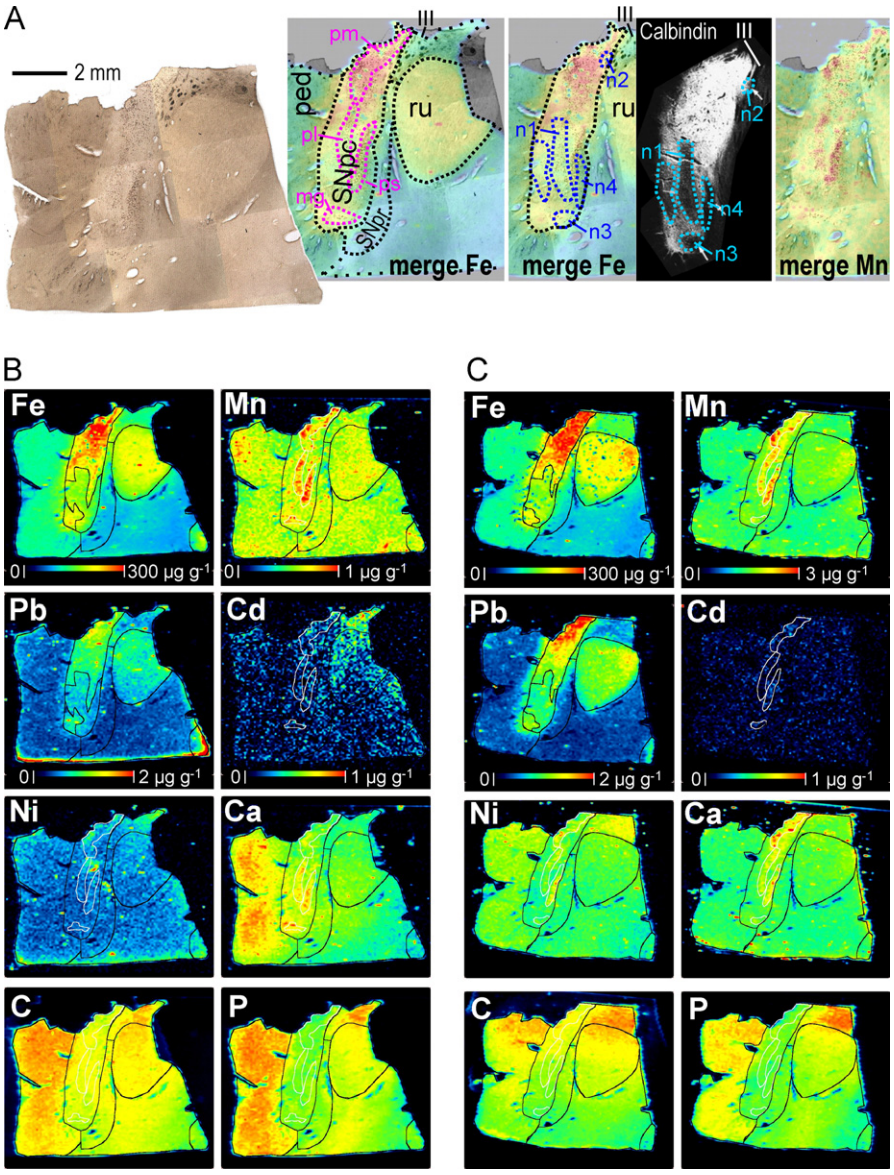

Fig. 2. (A; left to right) Photomicrograph of the unstained section 1 of human mesencephalon; overlay with the concentration map of Fe and subdivision according to [19]; overlay with the concentration map of Fe and approximate subdivision according to [20]; calbindin binding in a corresponding plain adapted from [20] for illustration; overlay with the concentration map of Mn. In the electronic version clusters of melanised cells (imposing as brown and black dots) and their congruence with the distribution of Mn but without congruence with the distribution of Fe can be distinguished at higher magnification. The concentration colour scales are the same as in (B). (B and C) Element images of sections 1 and 2 with contours overlaid as explained in (A). The images were obtained from the ion images of $^{56}Fe^+$, $^{208}Pb^+$, $^{111}Cd^+$, $^{60}Ni^+$, $^{44}Ca^+$ and $^{13}C^+$.

native tissue such as 109–199 $\mu g\,g^{-1}$ determined by instrumental neutron activation analysis (INAA) in 17 subjects of 17–90 years of age [5], 179 $\mu g\,g^{-1}$ determined by total reflection X-ray fluorescence spectrometry (TRXRF) in a 65-year-old subject [17], $135 \pm 12\ \mu g\,g^{-1}$ in formalin fixed tissue of 12 subjects (average age 70 years) determined by atomic absorption spectrometry [18] and $163 \pm 18\ \mu g\,g^{-1}$ in $n = 3$ by ICP-AES [6]. In white matter we measured 120 $\mu g\,g^{-1}$ which is in good accordance with literature values of 127 $\mu g\,g^{-1}$ [17]. The distribution pattern of Fe determined by LA-ICP-MS imaging was congruent to that observed by Popescu et al. [2] using synchrotron X-ray fluorescence.

With respect to Fe speciation, Mössbauer spectrometry studies on frozen human SN pointed to the majority of Fe being present as Fe(III) complexes in octahedral configuration within ferritin-like Fe-oxyhydroxyde clusters. This structure is contained in the species neuromelanin, ferritin and hemosiderin. The combination with instrumental neutron activation analysis, enzyme linked immunosorbent assays (ELISAs) and proteolytic fractionation studies on homogenates of human SN revealed that 10–20% of Fe was present as NM mostly in neurons, and the rest as ferritin and hemosiderin, mostly in glia [5]. Apparently, only a minimal fraction of Fe was present as heme complexes. All these Fe complexes have in common an extremely low solubility in pH-neutral solutions.

In view of these considerations, it is very plausible that the Fe concentrations measured here are close to the initial natural values. However, a potential wash-out of Ca, Fe, Mn or Pb has to be verified by comparative LA-ICP-MS measurements of native sections and sections stored in formalin from the same tissue block.

From previous studies we know that (i) heavy metals to which brain tissue had been exposed post mortem tend to bind preferentially to white matter [8], a phenomenon which is also well known from Os and U counterstains frequently used in electron microscopy and (ii) Pb is enriched in gray matter in native cryopreserved human brain [12]. Therefore it seems impossible that Pb which is specifically present in the SN and the NR results from external contamination. Concentrations of $3.0 \pm 0.4\ \mu g\,g^{-1}$ were reported 1989 in the SN of an urban population of $n = 9$ compared to 0.8 $\mu g\,g^{-1}$ measured here.

Mn imaging showed some deviation of the concentrations in the two measurements – amounting to 0.6 and 1.7 $\mu g\,g^{-1}$ in SN – due to lower count rates and higher background in section 1 but yielded the same distribution pattern. In the SN Mn concentrations of $0.7 \pm 0.2\ \mu g\,g^{-1}$ ($n = 12$) [18] and $0.4 \pm 0.1\ \mu g\,g^{-1}$ ($n = 9$) [6] were reported in the literature.

3.3. Anatomical architecture of element distributions

To further anatomically parcel out the SNpc into subregions, criteria have been established based onto the pattern of melanised neurons as appearing in light microscopy of unstained sections. The nomenclature proposed by Braak and Braak differentiated a posterolateral, a posteromedial, a posterosuperior and a magnocellular subnucleus (pl, pm, mg, ps) [19].

A scheme based on immunohistochemical stainig for the protein calbindin has been proposed by Damier et al. promising independence of degenerative neuronal demise. From a calbindin-rich matrix five calbindin-poor pockets termed nigrosomes were discriminated [20].

These subdivisions are of pathophysiological relevance as (e.g., in Parkinson's disease stages 3–6) several studies point to a specific time course of nigral degeneration starting in the posterior inferior regions and proceeding to the more anterior and dorsal areas of the SNpc.

Both types of subdivisions – which are not congruent – were applied to the present sample as illustrated in Fig. 2 and reported in Table 1. As no calbindin immunocytochemistry was performed in this study, a picture of a corresponding plane was adapted from [20] for illustrative purpose and the contours overlaid onto a Fe map. Nigrosome 5 was localized in a more superior plain and was not crossed in the present section.

The distribution of Ca and Mn (Fig. 2B and C) was highly congruent to that of melanised neurons reflecting the partition into subnuclei with similar concentrations throughout subnuclei. In this context it is of interest, whether Ca and Mn are subdued to degenerative processes similar to Fe or can serve as landmarks independent from degeneration.

In contrast, Fe and Pb rather reflected the matrix-nigrosome partition with clearly higher concentrations in the calbindin-rich matrix essentially located in the anterior part of the SNpc in the plains examined, congruent with [2]. Studies such as [2] also suggest that the increase in Fe in Parkinson's disease essentially takes place in the posterior rather nigrosomal compartment.

4. Conclusion

In conclusion, specific distribution patterns of Fe, Pb, Mn and Ca were preserved after more then 10 years of storage in formalin solution. Our data suggest that a meaningful anatomical and quantitative assessment of Fe, Mn and Pb is possible in this type of samples using LA-ICP-MS imaging. Fresh tissue is necessary for Zn and Cu determinations.

Acknowledgements

We thank Prof. Dr. Heiko Braak, Clinical Neuroanatomy, Dept. of Neurology, Clinical Research Centre, University of Ulm, 89081 Ulm, Germany, for kindly providing this very well staged and characterized sample material and fruitful discussion. The technical assistance of Astrid Zimmermann, is thankfully acknowledged.

References

[1] J. Stauber, R. Lemaire, J. Franck, D. Bonnel, D. Croix, R. Day, M. Wisztorski, I. Fournier, M. Salzet, MALDI imaging of formalin-fixed paraffin-embedded tissues: application to model animals of Parkinson disease for biomarker hunting, J. Proteome Res. 7 (2008) 969–978.
[2] B. Popescu, M. George, U. Bergmann, A. Garachtchenko, M. Kelly, R. McCrea, K. Lüning, R. Devon, G. George, A. Hanson, S. Harder, L. Chapman, I. Pickering, H. Nichol, Mapping metals in Parkinson's and normal brain using rapid-scanning X-ray fluorescence, Phys. Med. Biol. 54 (2009) 651–663.
[3] B.A. Faucheux, M.E. Martin, C. Beaumont, J.J. Hauw, Y. Agid, E.C. Hirsch, Neuromelanin associated redox-active iron is increased in the substantia nigra of patients with Parkinson's disease, J. Neurochem. 86 (2003) 1142–1148.
[4] A. Ektessabi, S. Yoshida, K. Takada, Distribution of iron in a single neuron of patients with Parkinson's disease, X-Ray Spectrom. 28 (1999) 456–460.
[5] L. Zecca, M. Gallorini, V. Schunemann, A.X. Trautwein, M. Gerlach, P. Riederer, P. Vezzoni, D. Tampellini, Iron, neuromelanin and ferritin content in the substantia nigra of normal subjects at different ages: consequences for iron storage and neurodegenerative processes, J. Neurochem. 76 (2001) 1766–1773.
[6] D.T. Dexter, F.R. Wells, A.J. Lees, F. Agid, Y. Agid, P. Jenner, C.D. Marsden, Increased nigral iron content and alterations in other metal ions occurring in brain in Parkinson's disease, J. Neurochem. 52 (1989) 1830–1836.
[7] J. Becker, Inorganic Mass Spectrometry: Principles and Applications, John Wiley and Sons, Cichester, 2007.
[8] J.S. Becker, J. Dobrowolska, M. Zoriy, A. Matusch, Imaging of uranium on rat brain sections using laser ablation inductively coupled plasma mass spectrometry: a new tool for the study of critical substructures affined to heavy metals in tissues, Rapid Commun. Mass. Spectrom. 22 (2008) 2768–2772.
[9] J.S. Becker, A. Matusch, C. Palm, D. Salber, K.A. Morton, S. Becker, Bioimaging of metals in brain tissue by laser ablation inductively coupled plasma mass spectrometry (LA-ICP-MS) and metallomics, Metallomics 2 (2010) 104–111.
[10] J.S. Becker, M. Zoriy, A. Matusch, B. Wu, D. Salber, C. Palm, Bioimaging of metals by laser ablation inductively coupled plasma mass spectrometry (LA-ICP-MS), Mass Spectrom. Rev. 29 (2010) 156–175.
[11] J.S. Becker, M.V. Zoriy, C. Pickhardt, N. Palomero-Gallagher, K. Zilles, Imaging of copper, zinc, and other elements in thin section of human brain samples (hippocampus) by laser ablation inductively coupled plasma mass spectrometry, Anal. Chem. 77 (2005) 3208–3216.

[12] J. Dobrowolska, M. Dehnhardt, A. Matusch, M. Zoriy, N. Palomero-Gallagher, P. Koscielniak, K. Zilles, J.S. Becker, Quantitative imaging of zinc, copper and lead in three distinct regions of the human brain by laser ablation inductively coupled plasma mass spectrometry, Talanta 74 (2008) 717–723.
[13] A. Matusch, C. Depboylu, C. Palm, B. Wu, G.U. Hoglinger, M.K. Schafer, J.S. Becker, Cerebral bioimaging of Cu, Fe, Zn, and Mn in the MPTP mouse model of Parkinson's disease using laser ablation inductively coupled plasma mass spectrometry (LA-ICP-MS), J. Am. Soc. Mass Spectrom. 21 (2010) 161–171.
[14] H. Braak, E. Braak, Neuropathological stageing of Alzheimer-related changes, Acta Neuropathol. 82 (1991) 239–259.
[15] H. Braak, K. Del Tredici, H. Bratzke, J. Hamm-Clement, D. Sandmann-Keil, U. Rüb, Staging of the intracerebral inclusion body pathology associated with idiopathic Parkinson's disease (preclinical and clinical stages), J. Neurol. 249 (2002) 1–5.
[16] J.C. Jurchen, S.S. Rubakhin, J.V. Sweedler, MALDI-MS imaging of features smaller than the size of the laser beam, J. Am. Soc. Mass Spectrom. 16 (2005) 1654–1659.
[17] L. Zecca, T. Shima, A. Stroppolo, C. Goj, G.A. Battiston, R. Gerbasi, T. Sarna, H.M. Swartz, Interaction of neuromelanin and iron in substantia nigra and other areas of human brain, Neuroscience 73 (1996) 407–415.
[18] R.J. Uitti, A.H. Rajput, B. Rozdilsky, M. Bickis, T. Wollin, W.K. Yuen, Regional metal concentrations in Parkinson's disease, other chronic neurological diseases, and control brains, Can. J. Neurol. Sci. 16 (1989) 310–314.
[19] H Braak, E. Braak, Nuclear configuration and neuronal types of the nucleus niger in the brain of the human adult, Hum. Neurobiol. 5 (1986) 71–82.
[20] P. Damier, E.C. Hirsch, Y. Agid, A.M. Graybiel, The substantia nigra of the human brain. I. Nigrosomes and the nigral matrix, a compartmental organization based on calbindin D(28K) immunohistochemistry, Brain 122 (Pt. 8) (1999) 1421–1436.